Characterisation of Rotary Friction Welding Process and Mechanism of Heat-Treated Scotch Pine

Jian Zhang, Wentao Fu, and Hai Zhu *

Rotary friction welding of wood to heat-treated lumber from Scotch pine is feasible and the strength of the joint exceeds that of glued and hammered joints. This study investigated the rotary friction welding process parameters and its welding mechanism applicable to heat-treated Scotch pine. Untreated Scotch pine served as the control. The one-way test revealed the tenon/bore ratio of 1.5, rotational speed of 2000 to 3500 r/min, and feed rate of 15 to 20 mm/s as the ideal process parameters for heat-treated Scotch pine. Under the same conditions, heat-treated material had weld strength up to 63.2% higher than untreated material. The portion of the weld zone with better weld strength was larger in size, had a full surface, and was darker in color, according to ultra-depth-of-field microscopic examinations. The internal wood components melted and cooled after the welding was finished and re-polymerized to form a tightly wrapped structure, linking the dowel rods to the substrate, according to the results of scanning electron microscopy.

DOI: 10.15376/biores.19.2.3793-3807

Keywords: Rotary friction welding of wood; Heat-treated Scotch pine; Process parameters; Welding effect; Welding Mechanism

*Contact information: College of Mechanical and Electrical Engineering, Northeast Forestry University, Harbin, China, 150040; *Corresponding author: endlesszhang@163.com*

INTRODUCTION

Wood is one of the finest options for replacing high-carbon emission materials such as plastics and steel in the context of a “dual-carbon” strategy because it is a naturally carbon-negative substance (Lu 2022). Wood welding is an environmentally friendly process technology, as it is glueless bonding, does not use metal connectors in the joining process, does not emit toxic substances, and is processed efficiently.

As early as 1996, Suthoff *et al.* (1996) published a patent for wood welding. Eco-friendly processing techniques such as those using renewable materials including wood may have significant advantages over their other counterparts with higher environmental burdens. Since 2003, Gfeller (2003) and Pizzi *et al.* (2004) have first started to investigate the physical phenomena involved in the wood welding process, where heat is generated by friction between the wood surfaces, leading to the melting of lignin and its flow to the weld line, which acts as a binder after cooling and solidification.

According to the movement trajectory of wooden components, there are now two main categories of wood friction welding technology: linear friction welding and rotating friction welding. Rotary friction welding involves inserting a dowel rod into a wooden substrate with a pre-drilled hole while rotating at a high speed. As a result of the heat produced, the lignin and hemicellulose in the wood melt and flow, and when the rotation stops, the molten polymer quickly cools and solidifies, joining the two pieces of wood. The entire process lasts only 3 to 5 s. It is important to note that the diameter of the pre-drilled holes should be smaller than that of the dowel bar, allowing for good friction between the dowel bar and the wood substrate (Suthoff *et al*. 1996; Gfeller *et al*. 2003, 2004; Pizzi *et al*. 2004).

In rotary friction welding, the influencing factors are the rotation and insertion rates of the dowel and the aperture ratio of the dowel to the pre-drilled holes in the wood substrate, the dowel form, the insertion angle, the welding time, and the type of wood, the grain direction, and the moisture content. Various factors also interact with each other. Wood species, dowel-to-substrate pre-drilled aperture ratio, and welding time are the three key factors that significantly affect the bond strength (Pizzi *et al*. 2004; Kanazawa *et al*. 2005), and dowel-to-substrate pre-drilled aperture ratio is the most critical factor (Ganne-Chédeville *et al*. 2005). For some European and North American woods, the weld strength is better at dowel rotation rates of 1000 to 1500 rpm (Rodriguez *et al*. 2010).

The wood weld strength is largely sufficient, but there is potential for improvement. Pretreating welding materials can increase the welding strength (Wang and Le 2019). Within specific bounds, it has been demonstrated that the addition of certain additives or other solutions (Pizzi *et al*. 2005; Mansouri *et al*. 2011; Amirou *et al*. 2017; Zhu *et al*. 2017) can improve weld strength. The process method can also be improved to increase weld strength. Some researchers have successfully employed bamboo dowel rods or bamboo nails in place of the original wooden dowel rods for rotational friction welding. When bamboo nails were used instead of wooden dowels and beech for rotary friction welding, the results showed that the adhesive strength of bamboo nails was higher than that of white latex (PVAc) and reached 6.42 MPa (Li *et al*. 2021). The test (Yang *et al*. 2022) showed that the temperature of the weld layer was higher when bamboo dowels were rotary friction welded and bamboo fibres were not easy to fracture, so higher pull-out strengths were obtained. The pull-out strength was 49.3% higher than that of rotary welding of wooden dowels.

Heat treatment of the wood substrate is another practical and environmentally friendly method that can be used to darken the color of the wood, preserve the color and texture of the logs, and overcome the problem that the surface layer of the logs is prone to linting without using any chemicals (Niu 2010). The pyrolytic treatment of wood using a high temperature (often 160 to 240 °C) for a specific amount of time is known as thermally modified wood, also known as charred wood and heat-treated wood in China (Gu *et al*. 2010). Heat-treated wood has been found to have good resistance to corrosion and pests, as well as reduced hygroscopicity, which increases its dimensional and shape stability, as well as increasing its dimensional and shape stability (Kubovský *et al*. 2020). Related articles (Boonstra *et al*. 2007; Roszyk *et al*. 2020) show the potential of heat-treated wood for applications in construction and in wet environments. A type of carbonized wood that is favored by many consumers who love wood items and are concerned about the environment in the home market is Scotch pine heat-treated timber. Heat-treated wood is more aesthetically pleasing than untreated wood, and it can be utilized completely for building decoration and outdoor gardens (Ma *et al*. 2009, 2011; Ding *et al*. 2015, Zhu *et al*. 2020; Zhang *et al*. 2021, 2023).

The amount of domestic and international research on the rotary friction welding process parameters for heat-treated Scotch pine is relatively small. By thoroughly studying the process parameters, it is possible to investigate the impact of various process parameters on the welding effect and mechanical properties as well as the laws governing their influence and to determine the ideal range of process parameters suitable for both heat-treated and untreated Scotch pine. In this study, a super depth-of-field microscope and a scanning electron microscope were used to compare the weld zone area of heat-treated and untreated wood. The variations in the weld zone area of various weld strengths were determined, and the variations in the internal organization of the wood before and after welding were analyzed. Variations in the timber's fiber structure were examined.

EXPERIMENTAL

Materials

The test was conducted using the same species of wood rotary friction welding. Heat-treated Scotch pine (Harbin province, China) was the test material, with the natural Scotch pine as the control material, and the base material and mortise and tenon bar were the same material. The welding substrate specimen size was 30 x 50 x 80 mm. The wood orientation was along the direction of the grain. The upper surfaces of the substrates were drilled with pre-drilled holes having diameters of 8 mm and depths of 50 mm. Tenon rod diameter specifications were 10 mm, 11 mm, 12 mm, and 13 mm. The length was 100 mm, and there was a chamfered tenon rod set up in front of the bar. The moisture content of the rods and the base material was adjusted to 6 to 12% to ensure the welding effect. The texture direction of the substrate is along the grain direction.

Rotary Friction Welding Test System for Wood

In Fig. 1a, the welding test bench is displayed. Prior to use, the substrate must be secured in a vise on the test bench and have pre-drilled holes made in it. To assure the quality of the welding, the substrate’s surface and the wood chips in the pre-drilled holes must also be thoroughly cleaned. The dowel bar is gripped with a jig and rotated at high speed by the spindle throughout the welding process. The feed rate and rotational speed of the dowel bar are adjustable from the console.

The mechanical properties of the specimen were tested according to GB/T 14018-(2009) to test the tensile strength of the rotary welded nodes of dowels and tenons, and the equipment adopts the specifications of the WDW100 Universal Mechanical Testing Machine. The specimens were loaded using a special fixture with a clamping length of approximately 40 mm at the upper end and the substrate at the lower end pressed against the surface of the fixture (Fig. 1b). The tensioning rate was 5 mm/min until the dowel bar was completely pulled out.

The post-weld specimen had dimensions of 20 x 20 x 2 mm (L x W x H). The welded tape area and the tissue characteristics of the welded and unwelded surfaces were observed in the microscope. The instrument was a Keyence VHX-2000 super depth-of-field 3D microscope.

To observe the organisation of the welded joints and welded interfaces and their changes before and after welding, the welded parts were examined with a sampling size of 15 x 15 x 5 mm (L x W x H). The samples were placed in a gold spraying box for metal spraying after being cleaned of any surface-level dust. The welding mechanism was then clarified by using a scanning electron microscope to examine the microstructural characteristics of the welded joints and welded interfaces as well as to compare the organizational changes before and after welding. The tool was a COXEM EM-30N scanning electron microscope.

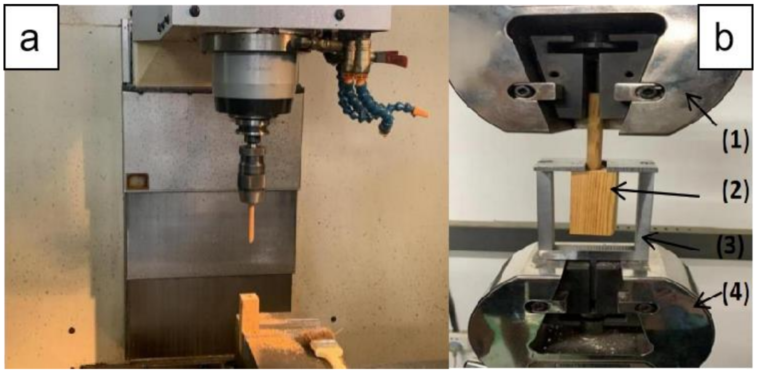

Fig. 1. Rotary friction welding test system. (a) Welding test rig; (b) Tensile test rig; (1) Tensile upper clamping block; (2) Wooden specimen; (3) Clamping fixture; (4) Tensile lower clamping block

Experimental Design

The strength comparison test of different wood joining methods was set up with welding test group, gluing test group, and knocking test group. For the welding test group, the 10 mm dowel rod was inserted into the 8 mm pre-drilled hole through high-speed rotation. The welding parameters were set speed 1500 rotations/min, feed speed of 15 mm/s, welding depth of 40 mm. For the gluing test group, there was 10.2 mm drill bit drilling out the pre-drilled holes, 10 mm dowel rods were inserted into the pre-drilled holes of 10.2 mm, through the gap fit, so that the actual size of the hole was always larger than the actual size of the shaft, to give the polyvinyl acetate grease outflow space. This was so that polyvinyl acetate grease evenly coated in the dowel rod can be inserted into the substrate and there would not be a large amount of overflow. The gluing depth was the same as the weld depth. For the knock test group, using a mallet, the 10 mm dowel rod was knocked into the 8 mm pre-drilled holes. The knock depth was the same as the weld depth. Each test group used 3 sets of specimens and the average was taken. To investigate the influence of process parameters on the weld strength of Scotch pine welded strip, a number of single-factor tests were designed to analyze and compare, and the single-factor tests were set up with tenon/bore ratio group, rotational speed group, and feeding speed group. The test program is shown in Table 1. For the one-factor test of tenon/bore diameter ratio, the fixed rotational speed was 2500 r/min, the feed speed was 15 mm/s, the tenon bar diameter varied from 10 to 14 mm, and a group of tests was made for every 1 mm change. Three specimens were tested in each group. For the one-way test of rotational speed, the fixed tenon/bore ratio was 12/8, the feed speed was 15 mm/s, the rotational speed varied from 1500 to 3500 r/ mm, and a group of tests was made for each change of 500 r/min. Again, 3 specimens were tested in each group. For the feed speed one-way test, the rotary speed was set at 3000 mm/s, the tenon to hole ratio was fixed at 12/8, the feed speed change range was 5 to 25 mm/s, and three specimens were tested for each group of tests after each change of 5 mm/s. Untreated Scotch pine was tested under the same program.

Table 1. Table of Factor Levels for One-Way Tests

Group	Considerations	Level				
		1	2	3	4	5
A	Tenon/Bore Ratio	10/8	11/8	12/8	13/8	
B	Rotation speed (r/min)	1500	2000	2500	3000	3500
C	Feed rate (mm/s)	5	10	15	20	25

RESULTS AND DISCUSSION

Comparative Analysis of Connection Strength in Hammering, Gluing, and Welding Tests

Under the same test conditions, the welded group, glued group, and knockout group were tested. In particular, the tensile pull-out resistance was tested with a specimen dowel bar diameter 10 mm, pre-drilled holes diameter 8 mm, depth of the same 50 mm, hammering, gluing, welding dowel bar insertion depth of 40 mm. Test results are shown in Table 2. It is clear that the connection strength of the welded group was much greater than that of the substrate and knockout groups. While obtaining a connection strength similar to that of the bonded group, the connection strength was improved by 216.8% for the substrate and by 202.4% for the knockout group. As can be observed, rotational friction welding successfully increased the joint strength of heat-treated Scotch pine. This process also confirms the efficiency and usefulness of friction welding wood.

Table 2. Comparison of Connection Strengths for Hammering, Gluing, and Welding Tests

Test Methods	Average (N)	Variation Coefficient	Max (N)	Min (N))
dowel rod	472	0.064	491.0	437.0
knockout test	494.5	0.046	512.0	468.5
gluing test	1448	0.150	1682.0	1252.5
welding test	1495.2	0.170	1784.0	1308.0

As shown in Fig. 2, the four curves overlapped at the beginning stage due to the pre-tensioning stage of the fixture, and after the pre-tensioning was over, the tensile curves of the welded and glued groups started to show obvious differences. Tensile performance tests were conducted on the welded specimens and the knocked specimens to obtain the typical change curves of force-displacement.

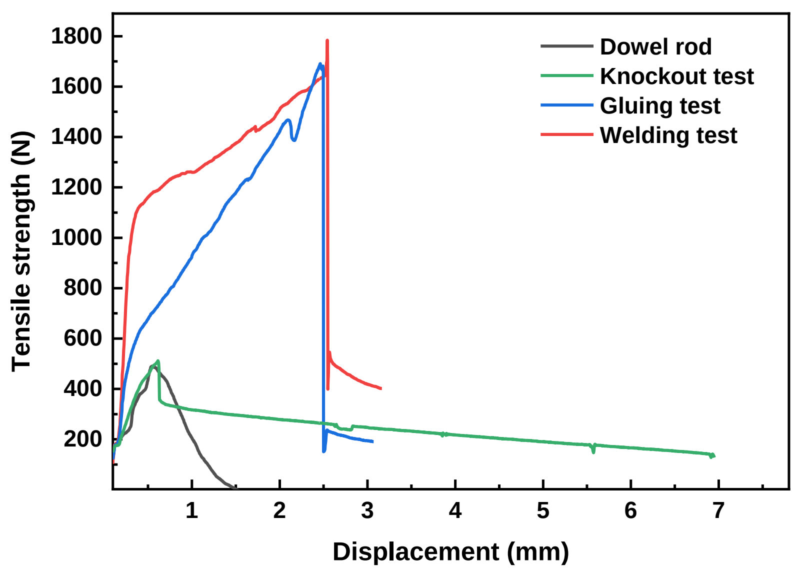

Fig. 2. Tensile strength-displacement curves of each group

The curves could be roughly split into three stages: the elastic rising stage, the yielding stage, and the extension and destruction stage. The welding and gluing group stages showed noticeable changes, while the substrate and knockdown group specimens showed more subtle changes. Hammering specimens to produce strength can be primarily attributed to mechanical interlocking of the rough peaks of the wood contact surface, elastic-plastic deformation of the microstructure, and static friction. Such aspects result in a low strength of the joint, quickly reaching the maximum tensile test force, followed by pull-out of mortise and tenon bars, and at this time the change in tensile force is not obvious when compared to the welded and glued groups. The breakdown of the connection interface causes a dramatic decline in the tensile force of the welded and glued specimens after a specific amount of time to reach the maximum tensile test force. While the tenon bar is being pulled out or destroyed, its tensile pull-out force also gradually decreases and tends to stabilize, even if the friction force is still present.

Analysis of the Influence of Process Parameters on Welding Results

For the tenon/aperture ratio group, in the experimental results shown in Fig. 3a, it was found that different tenon/aperture ratios had a significant effect on the weld strength. The tensile strength of the specimens of heat-treated Scotch pine was significantly higher than that of the untreated specimens, with a maximum increase of 31.1%. The tensile strength increased with the rise in the tenon/hole ratio and peaked at the ratio of 1.5 before progressively declining afterward. This was according to the curves of the heat-treated wood, which showed an increasing and then decreasing trend. The untreated Scotch pine material's curve trend matched that of the heat-treated material. The two laws were similar because, within a certain range, the larger the difference between the diameters of the tenon bar and the pre-drilled holes, the quicker the weld temperature is reached and the closer the conductive inter-cellular lignin flow is, providing more weld material for the weld. This is the reason for the similarity of the two laws. The tenon/hole ratio reached 1.625 at which point the tensile pullout strength of the camphor pine heat-treated and untreated material started to trend downward due to the increasing lateral pressure between the walls of the holes. This shows that the increase in the tenon/hole ratio is beneficial to improve the welding strength, but not unlimited expansion. The likelihood of the wood substrate breaking also increases, so the size of the substrate must be appropriately taken into account when designing the tenon/hole ratio.

For the rotational speed group, as shown in Fig. 3b, the tensile strength of the heat-treated Scotch pine material was also significantly higher than that of the untreated material for different rotational speeds, with a maximum increase of 53.3%, at a tenon/bore diameter ratio of 12/8 and a feed rate of 15 mm/s. For heat-treated materials, rotational speeds in the range of 2500 to 3500 r/min gave good welding results. For untreated materials, welding results were better in the range of 2500 to 3000 r/min. The efficacy of rotary friction welding wood depended on the selection of the rotational speed. Too high of a rotational speed may cause excessive carbonization or volatilization of the weld layer material, altering the mechanical properties of the weld layer and lowering the tensile strength. Too low of a rotational speed may result in insufficient welding and poor results. Therefore, in a real application, it is important to select the proper rotating speed based on the various tree species to improve the performance of the welded joint.

Due to the choice of a more suitable tenon ratio and rotational speed for the feed speed group, the increase in tensile strength of the specimens after heat treatment reached a maximum of 61.2%, as shown in Fig. 3c. When welding heat-treated specimens, a good welding effect can be obtained with a feed speed of 15 to 20 mm/s; when welding untreated specimens, a feed speed of 15 mm/s is sufficient. The heat-treated material's tensile strength showed that it increased with the increase in feed rate, peaked at 20 mm/s, and then started to decline. The tensile strength of the untreated specimens also increased with the increase in feed rate, peaked at 15 mm/s, and then gradually decreased in the range of 20 to 25 mm/s. The heat-treated specimens' higher tensile strength than the heat-treated specimens was also demonstrated by the tensile strength of the heat-treated specimens. As a result, up to a point, raising the feed rate might enhance the pull-out resistance of welded joints, but going over that point may compromise the weld's quality. Too low a feed rate prolongs the welding time and affects the curing of the weld layer, leading to poorer weld results and lower pull-out resistance. Too fast a feed rate may lead to inadequate welding, reduced weld area, and lower pull-out resistance. Furthermore, raising the feed rate raises the heat input, which could result in higher residual stresses and crack flaws during the welding process, impacting the final welding outcome.

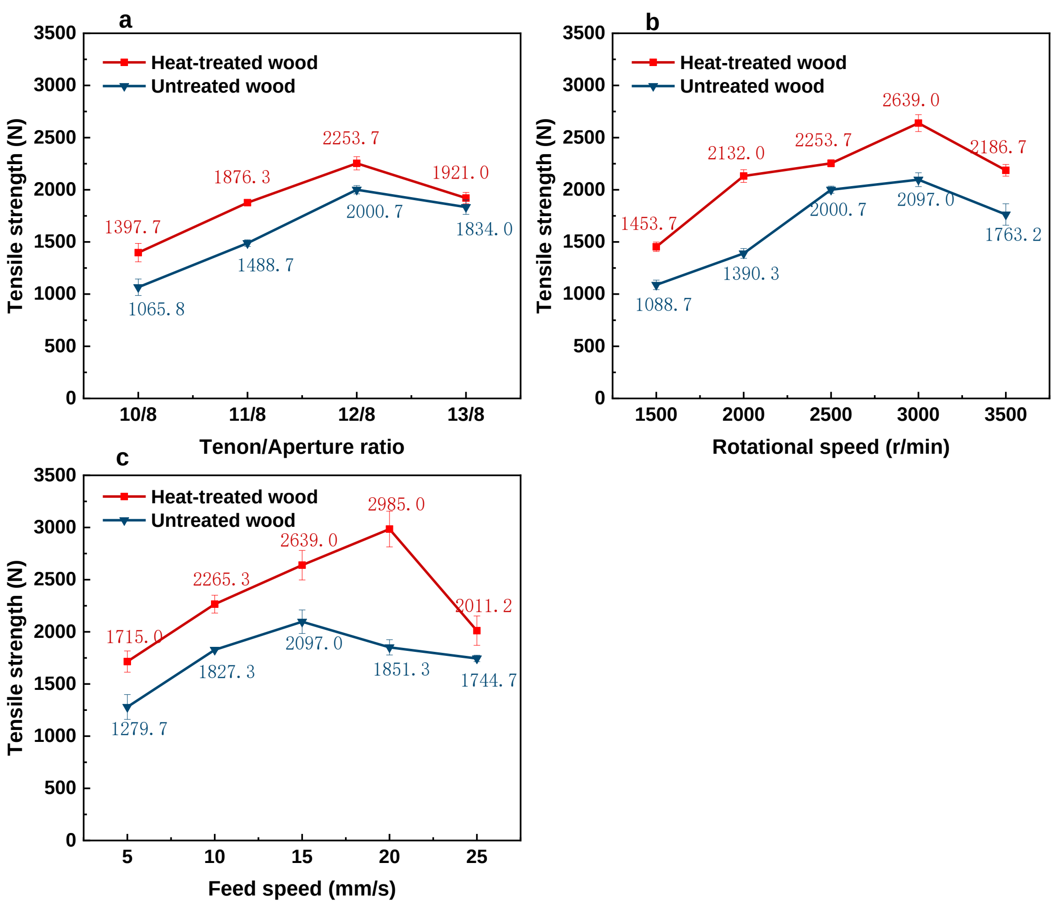

Fig. 3. Curves showing the influence of process parameters on the pullout strength

In summary, it is not difficult to see that after heat treatment of Scotch pine timber, the better range of process parameters also changed, which may be due to changes in the nature of the wood in the heat treatment process. The heat treatment may be changing the crystal structure of the wood, fibre arrangement, and moisture content and other physical properties. This may result in better plasticity and toughness, which affects the heat conduction, deformation, and stress distribution in the weld, and the internal residual stresses in the wood. Residual stresses within the wood may be reduced or more uniformly distributed, thus affecting the range of preferred process parameters.

Macro-morphological Analysis of Dowel Rods

The appearances of the extracted rods in each one-factor test group are shown in Fig. 4, and there was a layer of black material, *i.e.*, the welded interface layer, on the surface of the extracted tenon rods. The tenon/aperture ratio groupings are A and A*. As the tenon/aperture ratio rose from A1 to A4 and A*1 to A*4, the weld reaction area grew and the weld interface's color darkened, while the front end of the tenon bar was gradually transformed from a rounded table shape to a cylindrical shape. However, when the tenon/aperture ratio is too large, there is excessive friction between the tenon rod and the substrate, which can result in the consumption of too many tenon rods, increasing the thickness of the weld layer, and increasing the lability of the weld. In contrast, when the tenon/aperture ratio is too small, there is insufficient friction between the tenon rod and the substrate, which can lead to poorer welding results, smaller welding areas, lighter.

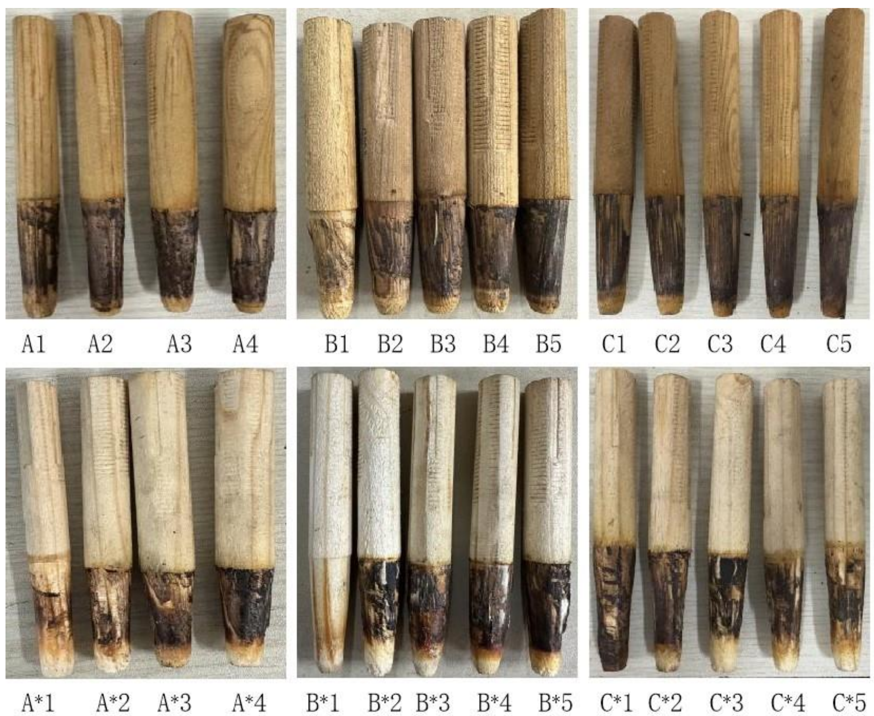

Fig. 4. Macro-morphological view of the welded joints of dowel rods.
A1-A4: tenon bars of heat-treated material tenon/bore ratio group, respectively 10/8, 11/8, 12/8, 13/8; B1-B5: tenon bars of heat-treated material rotational speed group, respectively 1500, 2000, 2500, 3000, 3500r/min; C1-C5: tenon bars of heat-treated material feed speed group, respectively 10, 15, 20, 25, 30 mm/s. A*, B*, C* are the tenon bars of untreated material under the same parameter, A*, B*, C* are the tenon bars of untreated material under the same parameter.

The groupings for rotational speed are B and B*. The extracted tenon bars in Groups B and B* had rounded front ends, indicating that the rotational speed had little bearing on how the tenon bars changed after welding and that the extraction of the tenon bars with wooden filaments was complete, indicating better welding results. From B1 to B5, it can be seen that the welded interface layer primarily exhibited the color of heat-treated material at low rotational speeds. However, as rotational speeds gradually increased, the color of the welded interface layer gradually changed to carbon black, deepened, and enlarged the area of the welded interface. Because Scotch pine itself included oily components and was smoother to the touch than at other rotational speeds, as can be seen from B*1, the untreated material was smooth and transparent at low rotating speeds. The color and size of the weld contact also deepened and expanded as the rotational speed rose. In contrast to heat-treated material, which had undergone a certain degree of carbonization after heat treatment, untreated material's color gradually shifted from light to burnt black and then to carbon black. As a result, the color of heat-treated material was darker than that of untreated material. The surface of the tenon bar exhibited apparent weld layer shedding at a rotational speed of 3500 r/min, with some spots exhibiting little white particles. When the rotational speed is too fast, the weld layer material may experience excessive carbonization, which affects the welding effect and results in a loss of mechanical properties, as shown by the tensile test; conversely, when the rotational speed is too slow, the feed resistance is greater, which results in insufficient welding, insufficient welding reaction, and frequently a poorer final welding effect.

Groups C and C* were tacho groups. The C1 and C*1 groups had the lowest feed rate, the longest welding time, the darkest welding interface color, and the largest welding reaction area. And it can be clearly seen that the size of the middle section of the tenon insertion part had been greatly reduced, which was due to the long-term friction between the tenon and the substrate, which produces a similar "cutting" effect. As the feed rate increased, the welding time became shorter, the area of the weld interface decreased, the colour of the weld interface layer became lighter, and the tenon bar became rounded. The findings of groups C and C* demonstrate that when the feed rate was too low, the welding time was extended, and the friction between the tenon bar and the wood substrate significantly reduced the tenon bar, causing a serious loss of tenon bar material and affecting the welding effect. Conversely, when the feed rate was too high, the welding reaction time was too short, the welding was insufficient, and the welded area was reduced, making the welding effect worse.

Analysis of the Observation Results of the Super-Depth-of-Field Microscope System

Unlike in the past, a super depth-of-field system was adopted to observe the weld zone, and the super depth-of-field map made it possible to observe the forming effect of the weld zone area very clearly. The Keyence VHX-2000 super depth of field three-dimensional microscope system was used to observe the welded strip of heat-treated and untreated material of Scotch pine. The details of the weld zone region were observed through the super depth of field micrographs, as shown in Fig. 5.

With appropriate welding parameters, the welding was good and the welded tape area was large. For instance, in Fig. 5c, the welded tape area takes up nearly all of the image, and the surface is flat and smooth. Changes in welding parameters caused changes in the morphology of the welded tape. On the other hand, when the welding was less efficient, the weld zone size was smaller, and it sometimes had flaws such as holes and depressions, which are likely to diminish the final weld strength. By comparing the micro-morphology of the weld zone area of the heat-treated and untreated materials, it was found that, under the same conditions, the weld zone of the untreated material exhibited a thinner state, the distribution of the weld zone is irregular, and the area of the weld zone area is not even close to that of the heat-treated material. As a result, the welded parts of the heat-treated material of the Scotch pine exhibit a higher weld.

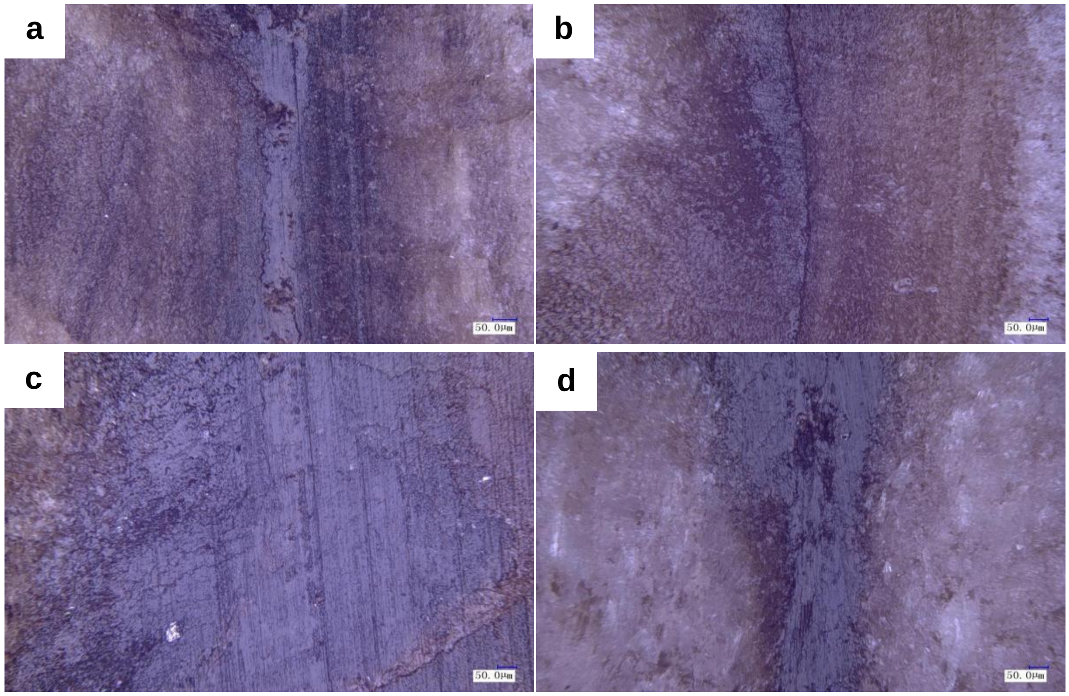

Fig. 5. Ultra-depth-of-field micrograph of the weld zone region. (a) Welding zone of heat-treated material at 1500 rpm; (b) Welding zone of untreated material at 1500 rpm; (c) Welding zone of heat-treated material at 3000 rpm; (d) Welding zone of untreated material at 3000 rpm

SEM Observations

By using a scanning electron microscope (SEM), the entanglement of tissues in the weld zone region can be seen. At a resolution of 10 µm, it is evident that after welding was complete, the molten wood components re-polymerised and entangled to form the weld zone interface, bonding the dowel rods to the substrate and giving the welded joints mechanical strength. It is demonstrated in Fig. 6 that the wood's softening and movement between its cells caused it to form a tightly wrapped shape when it was cooled.

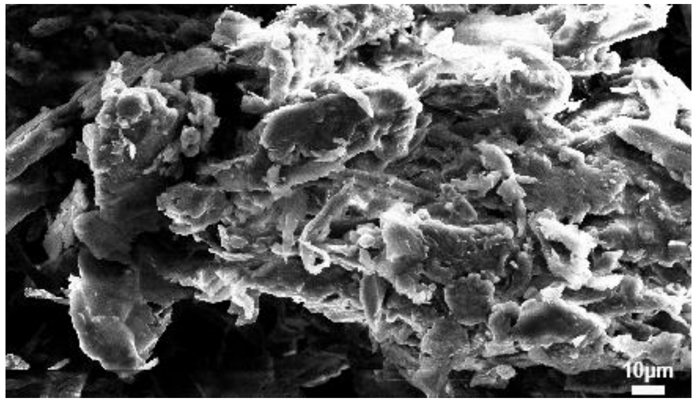

Fig. 6. Cooling of flowing wood components fixed in the structure of cellulose

The front end of the dowel bar after welding was sampled for observation, with a sample size of 15 x 15 x 5 mm. Figure 7a shows the welded surface profile of the head of the sampled dowel bar of untreated lumber and part c shows the welded surface profile of the head of the sampled dowel bar of heat-treated lumber. It is apparent from part c that a large area of welded tape was adhered to the surface of the dowel bar. The fibers on the surface of the dowel rod were welded to the fibers on the wall of the hole when magnified 200 times, as illustrated in Figs. b and d, and the fibers on the two surfaces are interwoven with one another in a nearly perpendicular pattern.

The welded band on the dowel bar made of the heat-treated material was thicker and denser when b and d were compared.

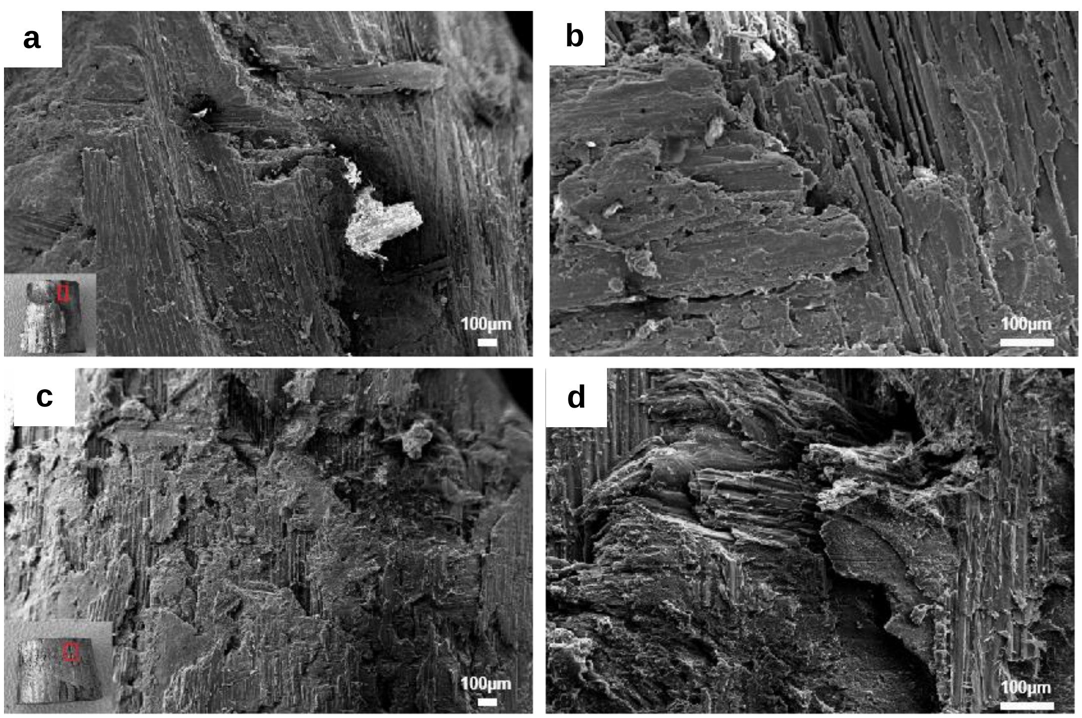

Fig. 7. Micro-morphology of the front end of the surface of the dowel bar of heat-treated and untreated wood from Scotch pine. (a) surface front profile of untreated material at low magnification; (b) surface front profile of untreated material at high magnification; (c) surface front profile of heat-treated material at low magnification; (d) surface front profile of heat-treated material at high magnification

Figure 8 illustrates the microscopic morphology of the welded surface at the bottom of the sampled dowel bar. Part 8e shows the topography of the welded surface of the bottom of the unheat-treated dowel bar, while Figure 8g shows the topography of the welded surface of the bottom of the sampled dowel bar that had been heat-treated. It is obvious that this area of the welded surface was flatter and denser, and it is possible to see clear signs of the flow of molten material after cooling. According to Figures f and h, a large number of entangled long wood cell fibers created a structure of entangled networks with the melt-cooled material when magnified 200 times. This was especially noticeable on the surface of the heat-treated dowel rods.

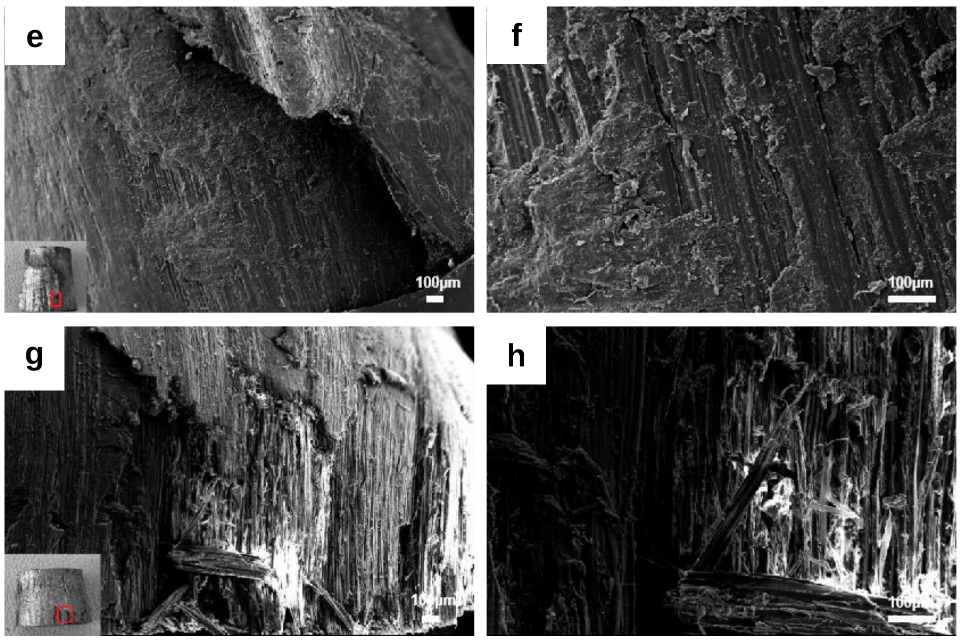

Fig. 8. Surface microscopic morphology of dowel rods of heat-treated and untreated wood of Scotch pine. Part (e) the bottom surface of untreated material at low magnification; (f) the bottom surface of untreated material at high magnification; (g) the bottom surface of heat-treated material at low magnification; (h) the bottom surface of heat-treated material at high magnification.

The signs of flow observed in these SEM images are evidence of temperature-induced softening and melting of wood intercellular material, revealing that the mechanism of rotational friction welding of wood is mainly through the friction of dowel rods against the substrate at high speeds, generating a large amount of heat, which results in the melting and flow of wood intercellular material. Eventually, these polymers cool down to form a welded interface that firmly "glues" the dowel bar to the substrate.

CONCLUSIONS

1. Rotary friction welding of heat-treated Scotch pine is feasible, and the strength of the wood weld under the same conditions exceeds the strength of the connection between knockdown and glued joints, verifying the effectiveness of wood welding.
2. A better range of process parameters for heat-treated and untreated materials was obtained by one-factor testing. The tenon/hole diameter ratio of 1.5, rotational speed in

the range of 2000 to 3500 r/min, and feed speed in the range of 15 to 20 mm/s was found to produce good welding results for heat-treated material; for untreated material, the tenon/hole diameter ratio of 1.5, rotational speed in the range of 2500 to 3500 r/min, and feed speed of 15 mm/s can produce good welding results. This is merely the value of one of the better process characteristics. To obtain the best welding strength, the test must be based on cooperation between all of the process parameters. Meanwhile, comparing the two materials reveals that, under the same parameters, the welded joint strength of the heat-treated material can be higher than that of the untreated material, with a maximum increase of 63.2%. This demonstrates that heat treatment enhances the weld joint strength of Scotch pine.

3. The "cutting" action between the dowel bar and the substrate during the welding process is affected by process parameterization, according to observation of the macroscopic morphology of the dowel bar surface. If the process parameters are not properly matched, the result can be insufficient friction between the dowel and the base material, leading to significant material loss of the wood dowel, resulting in a poor final welding outcome.

4. The welded area was observed using a super depth-of-field 3D optical microscopy system and SEM. The results from the super depth-of-field microscopy showed that, under the same parameters, the area of the welded region in the heat-treated Scots pine material was larger and the surface was smoother and more even. This may be one of the reasons why the heat-treated Scots pine material exhibited higher weld strength compared to untreated material. Observation with a scanning electron microscope revealed that the molten wood cells were linked together to form a welded band interface, which demonstrated the softening and flow between wood cells during the welding process and the formation of a tightly wound structure after cooling.

REFERENCES CITED

Amirou, S., Pizzi, A., and Delmotte, L. (2017). "Citric acid as waterproofing additive in butt joints linear wood welding," *European Journal of Wood and Wood Products* 75(4), 651-654. DOI: 10.1007/s00107-017-1167-x

Boonstra, M. J., VanAcker J., and Tjeerdsma, B. F. (2007). "Strength properties of thermally modified softwoods and its relation to polymeric structural wood constituents," *Annals of Forest Science* 64(7), 679-690. DOI: 10.1051/forest:2007048

Ding, T., Gu, L. B., and Cai, J. B. (2015). "Effect of heat treatment on hygroscopic properties and dimensional stability of wood," *Journal of Nanjing Forestry University (Natural Science Edition)* 39(02), 143-147. DOI: 10.3969/j.ssn.1000-2006.2015.02.025

Ganne-Chédeville, C., Pizzi, A., and Thomas, A. (2005). "Parameter interactions in two-block welding and the wood nail concept in wood dowel welding," *Journal of Adhesion Science and Technology* 19(13-14), 1157-1174. DOI: 10.1163/156856105774429037

GB/T 14018 (2009). "Test method for nail grip strength of wood," Standardization Administration of China, Beijing, China.

Gfeller, B., Properzi, M., and Zanetti, M. (2004). "Wood bonding by mechanically-induced *in situ* welding of polymeric structural wood constituents," *Journal of*

Applied Polymer Science 92(1), 243-251. DOI: 10.1002/app.13648
Gfeller, B., Zanetti, M., and Properzi, M. (2003). "Wood bonding by vibrational welding," *Journal of Adhesion Science and Technology* 17(11), 1573-1589. DOI: 10.1163/1568561041588192
Gu, L. B., Tu, D. Y., and Yu, X. L. (2007). "Characteristics and applications of charred wood," Chinese Wood-based Panel 05, 30-32+37. DOI: 10.3969/j.issn.1673-5064.2007.05.011
Kanazawa, F., Pizzi, A., and Properzi, M. (2005). "Parameters influencing wood-dowel welding by high-speed rotation," *Journal of Adhesion Science and Technology* 19(12), 1025-1038. DOI: 10.1163/156856105774382444
Kubovský, I., Kačíková, D., and Kačík, F. (2020). "Structural changes of oak wood main components caused by thermal modification," *Polymers* 12(2), article 485. DOI: 10.3390/polym12020485
Li, S. X., Zhang, H. Y., Cheng, L. S., Ju, Z. H., and Lu, X. N. (2021). "Study on the performance of high-speed rotary friction welding of moso bamboo pins (nails)," *Journal of Northwest College of Forestry* 36(04), 225-232+248. DOI: 10.3969/j.issn.1000-2006.2015.05.022
Lu, Y. (2022). "Supramolecular science of wood: Scientific significance and perspectives," *Wood Science and Technology* 36(02), 1-10. DOI: 10.12326/j.2096-9694.2022026
Ma, X. X., Jiang, M. L., and Lv, H. M. (2009). "Evaluation of corrosion resistance of heat-treated lumber of Sphagnum pine," *Timber Industry* 23(05), 45-47. DOI: 10.3969/j.issn.1001-8654.2009.05.013
Ma, X. X., Jiang, M. L., and Lv, H. M. (2011). "Evaluation of the durability of heat-treated lumber of Sphagnum pine," *Timber Industry* 25(01), 44-46. DOI: 10.3969/j.issn.1001-8654.2011.01.013
Mansouri, H. R., Pizzi, A., and Leban, J. M. (2011). "Causes for the improved water resistance in pine wood linear welded joints," *Journal of Adhesion Science and Technology* 25(16), 1987-1995. DOI: 10.1163/016942410X544794
Niu, X. Y. (2010). "Characteristics and applications of wood charring," *Furniture and Interior Decoration* 12, 96-97. DOI: CNKI:SUN:JJZS.0.2010-12-035
Pizzi, A., Leban, J. M., and Kanazawa, F. (2004). "Wood dowel bonding by high-speed rotation welding," *Journal of Adhesion Science and Technology* 18(11), 1263-1278. DOI: 10.1163/1568561041588192
Pizzi, A., Leban, J. M., and Zanetti, M. (2005). "Surface finishes by mechanically induced wood surface fusion," *Holz als Roh-und Werkstoff* 63(4), 251-255. DOI: 10.1007/s00107-004-0569-8
Rodriguez, G., Diouf, P., and Blanchet, P. (2010). "Wood-dowel bonding by high-speed rotation welding—Application to two Canadian hardwood species," *Journal of Adhesion Science and Technology* 24(8-10), 1423-1436. DOI: 10.1163/016942410X501025
Roszyk, E., Stachowska, E., and Majka, J. (2020). "Moisture-dependent strength properties of thermally-modified *Fraxinus excelsior* wood in compression," *Materials* 13(7), article 1647. DOI: 10.3390/ma13071647
Suthoff, B., Schaaf, A., Hentschel, H., and Franz, U. (1996). German Patent No. DE 196 20 273 C2.

Wang, J., and Le, H. (2019). "Research progress in friction welding technology for wood," *Journal of Northwest College of Forestry* 34(06), 191-196+258. DOI: 10.3969/j.issn.1001-7461.2019.06.30

Yang, H. D., Wang, N., Meng, X. M., Zhu, X. D., and Gao, Y. (2022). "Bamboo tenon rotary welding process parameters and mechanism investigation," *Journal of Beijing Forestry University* 44(02), 141-150. DOI: 10.12171/j.1000−1522.20210288

Zhang, J., Fu W. T., and Zhu, H. (2023). "Exploration and progress of wood friction welding technology," *China Adhesives* 32(08), 60-68. DOI: 10.13416/j.ca.2023.08.010

Zhang, J., Zhu, H., and Chen, J. Y. (2021). "Response surface analysis of the factors affecting the tensile pullout resistance of rotary welded dowels," *Forest Industry* 58(08), 25-29. DOI: 10.19531/j.issn1001-5299.202108005

Zhu, H., Chen, J. Y., and Zhang, J. (2020). "Factors affecting the pull-out resistance of rotary friction welding of wooden dowels," *Journal of Northeast Forestry University* 48(06), 75-79. DOI: 10.13759/j.cnki.dlxb.2020.06.016

Zhu, X. D., Zhang, J. R., Wu, Y., Ding, Q. F., and Gao, Y. (2017). "Effect of CuCl_2 treatment on the weldability of dowels," *Journal of Northwest College of Forestry* 32(06), 264-269. DOI: 10.3969/j.issn.1001-7461.2017.06.42

Article submitted: February 20, 2024; Peer review completed: March 16, 2024; Revised version received: March 19, 2024; Accepted: April 9, 2024; Published: April 26, 2024.
DOI: 10.15376/biores.19.2.3793-3807